

Inelastic diffractive-dissociation cross section in π^-p interactions at 200 GeV/c

J. W. Lämsä,* W. D. Walker, L. R. Fortney, A. T. Goshaw, J. S. Loos,[†] and W. J. Robertson
Duke University, Durham, North Carolina 27706

B. M. Schwarzschild, G. Hartner, G. Levman,[†] V. A. Sreedhar, and T. S. Yoon
University of Toronto, Toronto, Ontario, Canada M5S 1A7

P. M. Patel
McGill University, Montreal, Quebec, Canada H3C 3G1

W. D. Shephard, J. M. Bishop, N. N. Biswas, N. M. Cason, P. D. Higgins, and V. P. Kenney
University of Notre Dame, Notre Dame, Indiana 46556

H. I. Miettinen[‡]
Stanford Linear Accelerator Center, Stanford University, Stanford, California 94305
 (Received 22 May 1978)

For nondiffractive π^-p interactions at high energy we find that the dependence of the cross section on charge multiplicity in each c.m. hemisphere exhibits Koba-Nielsen-Olesen scaling. We use this behavior to extract a cross section for diffractive excitation of 3.4 ± 0.2 mb at 200 GeV/c. We attribute $\sim 55\%$ of this to pion excitation, with a mean breakup charge multiplicity of ~ 2.9 , $\sim 30\%$ to proton excitation, with mean charge multiplicity ~ 2.2 and $\sim 15\%$ to double excitation. We believe this technique is widely applicable for extracting the diffractive component in hadronic interactions.

It is of interest to determine the cross sections for diffractive dissociation of different hadrons in high-energy collisions. One can attempt this by looking for prominent departures, of diffractive origin, from smooth regularities of the nondiffractive component. We report here an application of such an approach to our 200-GeV/c π^-p data. Our technique, which is a novel generalization of ideas put forward by Sivers and Thomas,¹ is the following: We classify all inelastic events by their charge multiplicities (n_F, n_B) in the forward and backward hemispheres. Since the (even, even) subset requires charge exchange between the two hemispheres, it is at high energies almost free of the diffractive component. Using this subset, and making the entirely reasonable assumption that the *nondiffractive* part of the (odd, odd) subset should interpolate smoothly the (even, even) subset, we separate the (odd, odd) subset into its nondiffractive and diffractive components. This separation is greatly facilitated by the important empirical observation that the (even, even) subset satisfies a modified form of Koba-Nielsen-Olesen (KNO) scaling.² In addition to its conceptual simplicity, the above technique represents a method for extracting the diffractive component which provides a useful alternative to the more conventional methods based on Feynman- x , missing-mass, or momentum-transfer cuts. In all of these methods it is necessary to estimate the contribution of a background of unknown form on which the diffractive component is superimposed; in the

method described here, no such background subtraction is required. Possible sources of error are thus expected to be quite different. Our estimates of errors suggest that this method based on forward-backward multiplicities should be at least as reliable as the conventional methods when applied to comparable data samples. A problem with the method, which may cause an underestimate of diffractive contributions at high charge multiplicities, is that some particles from decays of diffractive systems of very high mass may occasionally cross over into the opposite hemisphere, thus contributing to the (even, even) subset which is assumed to represent a purely nondiffractive component. We note, however, that difficulties in estimating diffractive contributions at large mass and high multiplicity are at least as serious for the other methods cited, since the signal-to-background ratio becomes quite small and the errors on the estimated diffractive signal are very large. In the kinematical region where diffractive and nondiffractive processes are both significant, they may even interfere. In such a situation it is difficult, if not impossible, to achieve a definitive separation with currently available statistics.

The analysis reported here is based on approximately 17 000 inelastic events of all topologies, obtained with a hybrid spectrometer composed of the Fermilab 30-in. bubble chamber and a wide-gap spark-chamber system. Details of the spectrometer can be found in Ref. 3.

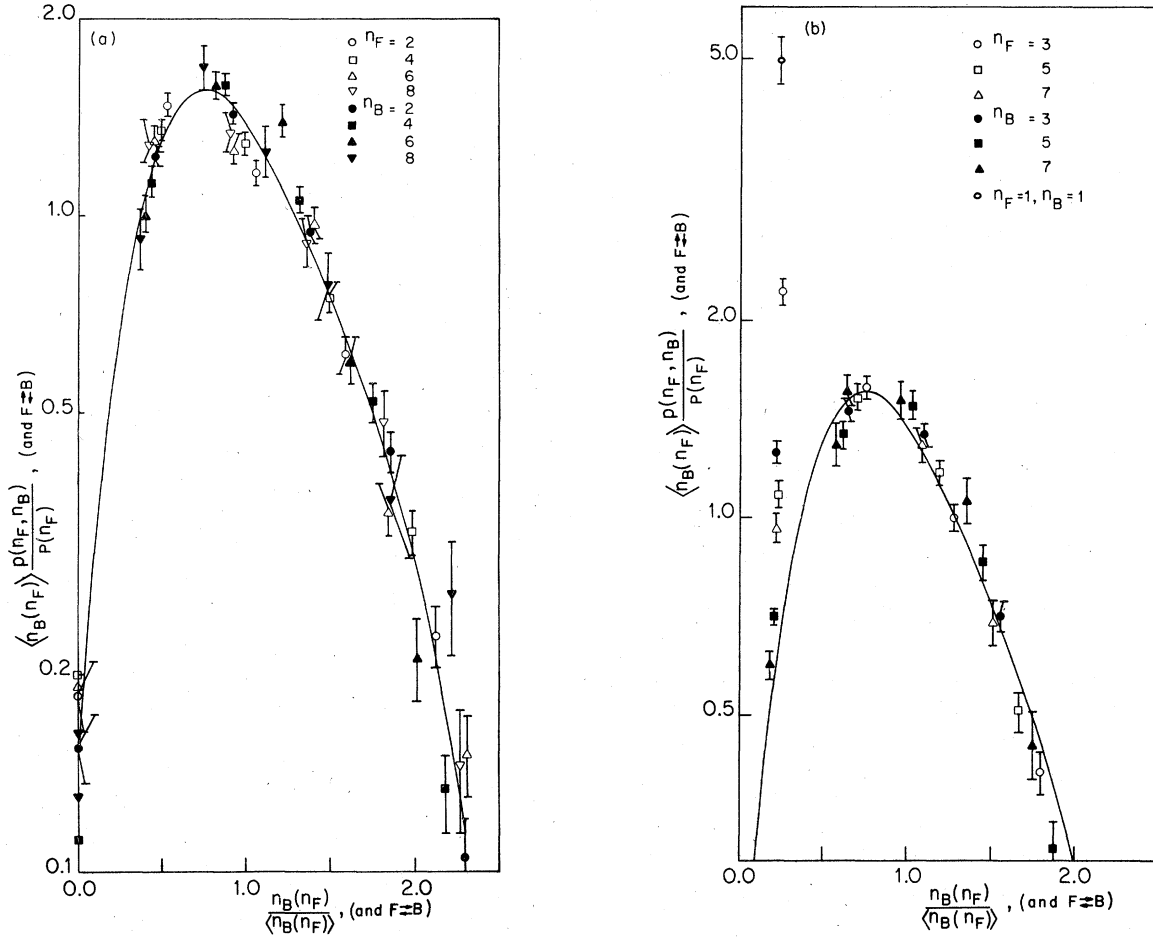


FIG. 1. (a) Distribution in the KNO-scaled c.m.-hemisphere charged-particle multiplicity, for a fixed even number of particles in the other hemisphere. The curve is a function fitted to the data. See text for a definition of the variables and of the fitted function. (b)

Same as above for a fixed odd number of particles. The data are fitted, excluding points with $n_F, n_B=1$, to the curve determined above. The $\langle n_B(n_F) \rangle$ are the nondiffractive means. The curve is the same in (a) and (b).

We define the following distribution functions and means:

$$\begin{aligned}
 p(n_F, n_B) &= \sigma(n_F, n_B) / \sigma_{\text{inelastic}}, \\
 p(n_F) &= \sum_{n_B} p(n_F, n_B), \\
 p(n_B) &= \sum_{n_F} p(n_F, n_B), \\
 \langle n_F(n_B) \rangle &= \sum_{n_F} n_F p(n_F, n_B) / p(n_B), \\
 \langle n_B(n_F) \rangle &= \sum_{n_B} n_B p(n_F, n_B) / p(n_F).
 \end{aligned}
 \tag{1}$$

Our first task is to find a suitable method for interpolating the cross sections of the (even, even) subset. Guided by the knowledge that the multi-

plicity distributions of inclusive as well as of many semi-inclusive processes exhibit KNO scaling,⁴ we plotted the quantity

$$\langle n_F(n_B) \rangle \frac{p(n_F, n_B)}{p(n_B)} \equiv f(z_{FB}, n_B)
 \tag{2}$$

versus z_{FB} , where $z_{FB} = n_F(n_B) / \langle n_F(n_B) \rangle$. Figure 1(a) shows this quantity, as well as the corresponding quantity with the roles of n_F and n_B reversed, for the even-even subset. We see that, to a good approximation, all the data points lie on a universal curve, i.e., the function $f(z_{FB}, n_B)$ equals $f(z_{BF}, n_F)$ and depends only on z and not on n . This empirical regularity,⁵ KNO scaling of the multiplicity distributions of individual hemispheres, is one of many empirical scaling properties of multiplicity distributions.

In order to estimate the nondiffractive part of

the (odd, odd) subset we fit the (even, even) data shown in Fig. 1(a) with a fourth-order power series

$$f(z) = \exp\left(\sum_{i=0}^4 a_i z^i\right), \quad z = z_{FB}, z_{BF} \quad (3)$$

obtaining the best fit ($a_i = -1.9, 8.0, -9.1, 4.1, -0.72$, for $i = 0, \dots, 4$), which is also shown in Fig. 1. The above function is chosen for its simplicity, and has no theoretical significance. Using this fit as the interpolating function, we then proceed to estimate the nondiffractive (odd, odd) cross sections. Here we face a small technical difficulty. In order to plot the (odd, odd) data in a fashion similar to that of Fig. 1(a), we need to know the various nondiffractive (ND) means $\langle n_F^{ND}(n_B \text{ odd}) \rangle$ and $\langle n_B^{ND}(n_F \text{ odd}) \rangle$, and none of these can be determined directly without knowing the diffractive admixtures in the (odd, odd) cross sections beforehand.

This problem can be tackled in several different ways. A straightforward approach is simply to assume that the (odd, odd) nondiffractive mean multiplicities $\langle n_B^{ND}(n_F) \rangle$ interpolate smoothly between $\langle n_B(n_F - 1) \rangle$ and $\langle n_B(n_F + 1) \rangle$. We have chosen instead to use the following alternative method based on the assumption of smooth variation and approximate KNO scaling for the forward-backward multiplicities in the nondiffractive component at all multiplicities. From earlier high-energy experiments, as well as from general factorization arguments, we know that the contribution of double-diffractive processes (i.e., of processes where both the beam and the target particles dissociate) into the cross sections $\sigma(\text{odd} > 1, \text{odd} > 1)$ is small. Neglecting this small admixture,⁶ we may fit the $\sigma(\text{odd} > 1, \text{odd} > 1)$ data directly to Eqs. (2) and (3), with the various $\langle n_F^{ND}(n_B \text{ odd} > 1) \rangle$ and $\langle n_B^{ND}(n_F \text{ odd} > 1) \rangle$ as the only free parameters, the parameters of Eq. (3) having been fixed by the (even, even) data. [See Fig. 1(a).] For example, $\langle n_F^{ND}(n_B = 5) \rangle$ is determined by fitting the data for $p(n_F > 1, n_B = 5)$ to Eq. (2). We can then deduce $p^{ND}(1, 5)$, and similarly the other $p^{ND}(1, n_B > 1)$ and $p^{ND}(n_F > 1, 1)$ from Eq. (2). The resulting nondiffractive and diffractive cross sections are given in Table I. To complete the task of determining the diffractive component, we need $p^{ND}(1, 1)$. To this end we use the $\sigma_{ND}(>1, 1)$ and $\sigma_{ND}(1, >1)$ to fit for $\langle n_F^{ND}(n_F = 1) \rangle$ and $\langle n_B^{ND}(n_B = 1) \rangle$ as above. Putting these in Eq. (2) gives us two independent determinations of the nondiffractive component of $\sigma(1, 1)$. It is reassuring to note in Table I that the two determinations come out quite close to one another.

Let us consider further the physical plausibility of this determination of the diffractive cross sections. In Fig. 2 (solid points) we see that at low

TABLE I. Cross sections for forward-backward multiplicities with either $n_F = 1$ or $n_B = 1$. The quoted errors include statistical errors and contributions from the fitting process but do not include any allowance for approximations made in determining the method of fitting.

(n_F, n_B)	$\sigma(n_F, n_B)$ (mb)	$\sigma_{ND}(n_F, n_B)$ (mb)	$\sigma_{diff}(n_F, n_B)$ (mb)
(1, 1)	1.47 ± 0.10	0.19 ± 0.03 0.18 from $p(n_F, 1)$ 0.20 from $p(1, n_B)$	1.28 ± 0.10
(3, 1)	1.53 ± 0.10	0.47 ± 0.09	1.06 ± 0.13
(1, 3)	0.94 ± 0.08	0.44 ± 0.08	0.50 ± 0.08
(5, 1)	0.71 ± 0.07	0.41 ± 0.08	0.30 ± 0.08
(1, 5)	0.36 ± 0.05	0.28 ± 0.06	0.08 ± 0.04
(7, 1)	0.33 ± 0.04	0.20 ± 0.06	0.13 ± 0.06
(1, 7)	0.13 ± 0.05	0.11 ± 0.05	0.02 ± 0.02
Total	5.47 ± 0.19	2.10 ± 0.18	3.37 ± 0.21

multiplicities the (odd, odd) hemisphere mean charge multiplicities are consistently lower than their (even, even) neighbors. This is no doubt due largely to diffractive dissociation. By contrast, the nondiffractive mean multiplicities deduced above (open circles) interpolate smoothly between their neighbors. It is interesting to note that the (odd, odd) mean multiplicities for the nondiffractive component derived by our method are quite consistent with those which would have been obtained by straight-line interpolation between adjacent (even, even) mean multiplicities. Any de-

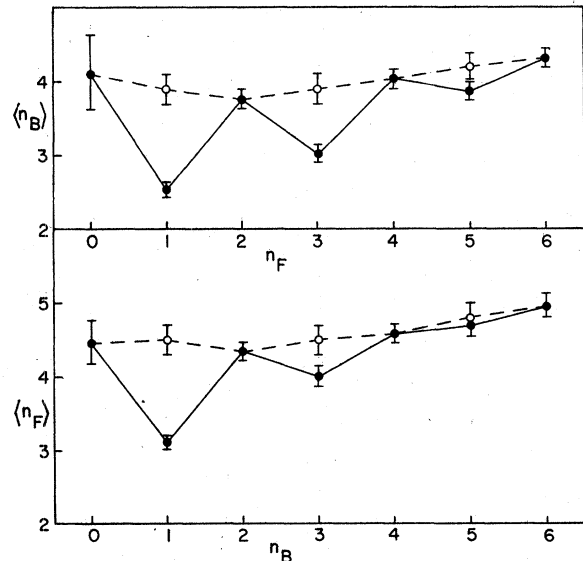


FIG. 2. The average c.m.-hemisphere charged multiplicity as a function of the charged multiplicity in the other hemisphere (solid points). The open points are fitted averages for the nondiffractive component (see text).

viations which occur seem to correspond to slightly higher (odd, odd) mean multiplicities than those estimated by simple interpolation. The differences, however, are not statistically significant. It is clear that an adequate estimate of the diffractive and nondiffractive components in the cross section can be obtained via the simpler method of interpolation for finding the nondiffractive (odd, odd) mean multiplicities.

We have used the calculated nondiffractive mean hemisphere multiplicities to plot in Fig. 1(b) the "raw" (odd, odd) distribution in the manner of Koba, Nielsen, and Olesen, with the scaling function f from Fig. 1(a) [fitted from (even, even) data] superimposed for comparison. We find that the same f describes the $\sigma(>1, >1)$ points reasonably well, whereas the points with one prong in either hemisphere rise in a striking fashion above f . We attribute this peak to diffractive dissociation, and the scaling background below it to nondiffractive processes.

Figure 3 compares the inelastic diffractive cross sections obtained in the above fashion with the nondiffractive cross sections as a function of charge multiplicity. (Data on the total charge multiplicity distribution from Ref. 7 have been used in this figure.) The total inelastic diffractive cross section is 3.4 ± 0.2 mb, which is approximately 16% of the total inelastic cross section. This is quite close to the elastic cross section of 3.18 ± 0.13 mb,⁷ just as is the case with pp scattering.⁸ The diffractive component is concentrated at low multiplicities, with a mean charge multiplicity of 3.6 ± 0.1 , compared to the nondiffractive component with a cross section of 17.6 ± 0.4 mb and a mean charge multiplicity of 8.8 ± 0.1 .

If we neglect double diffractive dissociation (see below) the $\sigma_{\text{diff}}(>1, 1)$ in Table I describe the diffractive breakup of the beam π^- , while $\sigma_{\text{diff}}(1, >1)$ describe the proton breakup. But the present analysis does not tell us how to allocate $\sigma_{\text{diff}}(1, 1)$ between beam and target excitation. However, in the case of 2-prong events, it is possible to make a good estimate of the beam diffractive breakup from a plot of mass recoiling against the proton using a background-subtraction method. With a straightforward (and *small*) background subtraction, we find the 2-prong cross section for diffractive excitation of the π^- to be 0.71 ± 0.05 mb.⁹ Subtracting this from our $\sigma_{\text{diff}}(1, 1)$ we get ~ 0.57 mb for the diffractive breakup of the target proton with only one charged track. Using these results, we can compare the cross sections and charge multiplicity distributions for pion and proton diffractive excitation. We obtain estimates for $\sigma_{\text{diff}}^{\pi}$ and σ_{diff}^p of 2.19 and 1.18 mb, respectively. The ratio $\sigma_{\text{diff}}^{\pi} / \sigma_{\text{diff}}^p$ is then ~ 1.9 . We find that the charge multi-

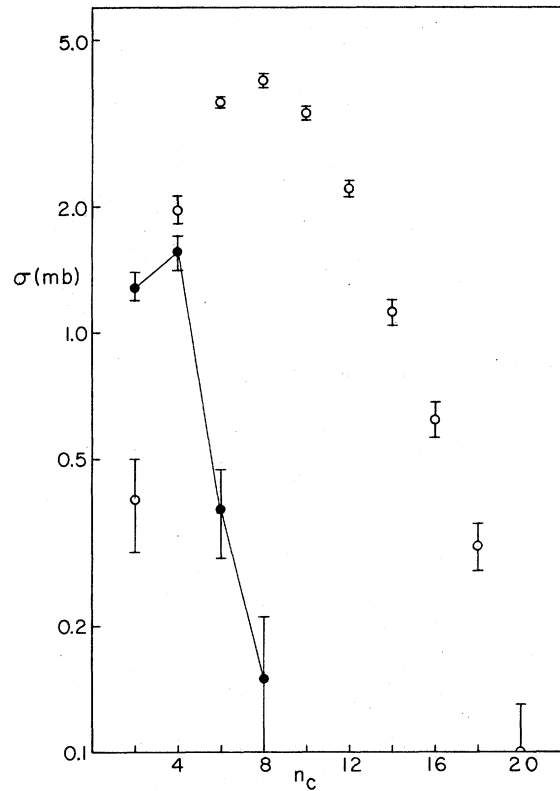


FIG. 3. The charged-particle multiplicity distribution for inelastic diffractive dissociation (solid circles) and for the nondiffractive component (open circles).

plicity for pion breakup tends to be higher ($\langle n_F \rangle^{\pi} \sim 2.9$) than for proton dissociation ($\langle n_B \rangle^p \sim 2.2$).

The above values of $\sigma_{\text{diff}}^{\pi}$ and σ_{diff}^p include possible contributions from double-diffractive-dissociation channels $\sigma_{\text{DD}}(>1, 1)$ and $\sigma_{\text{DD}}(1, >1)$ in addition to the true single-diffractive cross sections. The size of these contributions can be estimated from factorization relations. If we ignore kinematic t_{min} effects,¹⁰ which are known to suppress double dissociation much more than single dissociation, we obtain the approximate relations

$$\sigma_{\text{DD}}(>1, 1) \approx \frac{\sigma_{\text{SD}}^{\pi}(>1, 1)\sigma_{\text{SD}}^p(1, 1)}{\sigma_{\text{el}}}, \quad (4a)$$

$$\sigma_{\text{DD}}(1, >1) \approx \frac{\sigma_{\text{SD}}^{\pi}(1, 1)\sigma_{\text{SD}}^p(1, >1)}{\sigma_{\text{el}}}, \quad (4b)$$

where σ_{SD} represents a true single-diffractive cross section. Similar relations may be written for the $\sigma_{\text{DD}}(\text{odd} > 1, \text{odd} > 1)$ cross sections. From these relations and the $\sigma_{\text{diff}}^{\pi}$ and σ_{diff}^p values previously obtained, it is possible to find a consistent set of estimates: σ_{DD} (all channels) ~ 0.4 – 0.5 mb

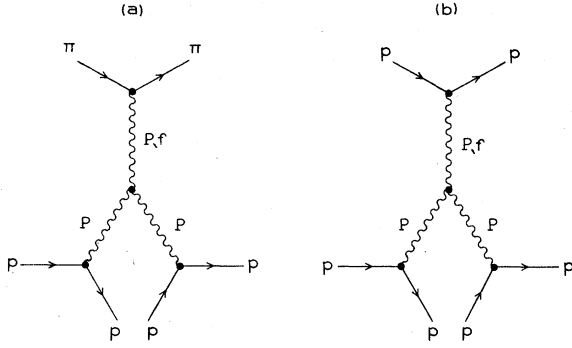


FIG. 4. Triple-Regge diagrams describing (a) pion diffractive dissociation in πp collisions and (b) proton diffractive dissociation in pp collisions. The inclusive cross section is given by a linear combination of the triple-Pomeron and PPf terms.

(<20% of σ_{diff}), $\sigma_{SD}^{\pi} \approx 1.9$ mb, and $\sigma_{SD}^p \approx 1.0$ mb. The ratio of $\sigma_{SD}^{\pi}/\sigma_{SD}^p$ remains ~ 1.9 .

Factorization may also be used to obtain an estimate of proton single-diffractive dissociation in proton-proton collisions. Consider the triple-Regge diagrams, shown in Fig. 4, describing pion dissociation in πp collisions and proton dissociation in pp collisions. Since the Pomeron and f couplings to the external particles are empirically known to be proportional to each other,¹¹ we get

$$\sigma_{SD}(pp) = 2\sigma_{SD}^{\pi}(\pi p) \frac{\sigma_{tot}(pp)}{\sigma_{tot}(\pi p)}. \quad (5)$$

Using the above value, $\sigma_{SD}^{\pi}(\pi p) = 1.9$ mb and the total-cross-section ratio 1.63 we obtain $\sigma_{SD}(pp) = 6.2$ mb, in good agreement with the various empirical estimates⁸ of 5 to 7 mb.

In summary, we find that Koba-Nielsen-Olesen scaling describes well the dependence of the non-diffractive cross section on the charge multiplicity in each c.m. hemisphere. We exploit this fact to estimate the cross sections for diffractive excitation of the π^- and proton by examining the departure from the scaling background. This method of isolating diffractive dissociation appears at least as reliable as standard methods now in use. We find a total inelastic diffractive-dissociation cross section $\sigma_{diff} = 3.4 \pm 0.2$ mb which is comparable to σ_{e1} . Pion dissociation accounts for $\sim 55\%$ of this and has mean charge multiplicity 2.9, while proton dissociation accounts for $\sim 30\%$ with a lower mean charge multiplicity 2.2. Double dissociation accounts for the remaining $\sim 15\%$ of σ_{diff} . Comparison of our results with pp data are in satisfactory agreement with factorization.

We wish to acknowledge the cooperation of the Fermilab staff and the help of our analysis and technical staffs. This work was supported in part by the U. S. Department of Energy, Division of Basic Energy Sciences, the National Research Council of Canada, and the National Science Foundation.

*Present address: Iowa State University, Ames, Iowa 50010.

†Present address: Argonne National Laboratory, Argonne, Illinois 60439.

‡Present address: Fermi National Accelerator Laboratory, Batavia, Illinois 60510.

¹D. Sivers and G. H. Thomas, Phys. Rev. D **9**, 208 (1974); **9**, 319 (1974).

²Z. Koba, H. B. Nielsen, and P. Olesen, Nucl. Phys. **B40**, 317 (1972).

³G. A. Smith, in *Particles and Fields—1973*, proceedings of the meeting of the Division of Particles and Fields of the APS, Berkeley, edited by H. H. Bingham, M. Davier, and G. R. Lynch (AIP, New York, 1973), p. 500.

⁴For a review, see J. Whitmore, Phys. Rep. **10C**, 273 (1974); **27C**, 187 (1976).

⁵The KNO scaling of multiplicity distributions in individual hemispheres was first reported by H. Grassler *et al.*, Nucl. Phys. **B90**, 461 (1975).

⁶An experimental justification for the neglect of double-diffraction contributions to the cross sections $\sigma(\text{odd} > 1, \text{odd} > 1)$ is found in the lack of deviation of the corresponding points from the curve in Fig. 1(b).

⁷D. Ljung *et al.*, Phys. Rev. D **15**, 3163 (1977).

⁸F. T. Dao *et al.*, Phys. Lett. **45B**, 399 (1973); S. J.

Barish *et al.*, Phys. Rev. Lett. **31**, 1080 (1973); J. W. Chapman *et al.*, *ibid.* **32**, 257 (1974); J. Benecke *et al.*, Nucl. Phys. **B76**, 29 (1974); M. G. Albrow *et al.*, *ibid.* **B103**, 1 (1976).

⁹P. D. Higgins, Notre Dame internal report (unpublished).

¹⁰In a process $a + b \rightarrow c + d$, the minimum momentum transfer is

$$|t_{\min}| = \frac{1}{s} (m_c^2 - m_a^2) (m_d^2 - m_b^2) + \frac{1}{s} (m_c^2 + m_d^2 - m_a^2 - m_b^2) \times \left(\frac{m_c^2 m_d^2}{s - m_c^2 - m_d^2} - \frac{m_a^2 m_b^2}{s - m_a^2 - m_b^2} \right)$$

In the single-excitation process, the first term vanishes. The second term is small, except when the mass of the excited system becomes very large ($M^2 \gtrsim 0.1 s$). In double excitation, the first term is nonzero and provides an effective damping of the cross section when the masses of both of the excited systems become simultaneously large. For further discussion of the t_{\min} effect and numerical estimates, see H. D. I. Abarbanel and G. L. Kane, Phys. Rev. Lett. **30**, 67 (1973); D. P. Roy and R. G. Roberts, Nucl. Phys. **B77**,

240 (1974).

¹¹The ratio of the Pomeron couplings is $\sigma_{\text{tot}}(p p) / \sigma_{\text{tot}}(\pi p) \approx \frac{4.95}{2.97} \approx 1.63$. From the total cross-section fits of Barger and Phillips [Nucl. Phys. B40, 205 (1972)] one ob-

tains for the ratio of the f couplings $4.95/2.97 \approx 1.66$. This proportionality of the Pomeron and f couplings is known as the “ f dominance of the Pomeron.”